Cell Tissue Res (2016) 363:461–478
DOI 10.1007/s00441-015-2253-1

REGULAR ARTICLE

Adipose tissue macrophages in non-rodent mammals: a comparative study

Grace Ampem[1] · Hind Azegrouz[2] · Árpád Bacsadi[3] · Lajos Balogh[4] · Susanne Schmidt[1] · Julianna Thuróczy[5] · Tamás Röszer[1]

Received: 24 March 2015 / Accepted: 3 July 2015 / Published online: 4 August 2015

Abstract The stromal vascular fraction (SVF) of adipose tissue in rodents and primates contains mesenchymal stem cells and immune cells. SVF cells have complex metabolic, immune and endocrine functions with biomedical impact. However, in other mammals, the amount of data on SVF stem cells is negligible and whether the SVF hosts immune cells is unknown. In this study, we show that the SVF is rich in immune cells, with a dominance of adipose tissue macrophages (ATMs) in cattle (*Bos primigenius taurus*), domestic goat (*Capra aegagrus hircus*), domestic sheep (*Ovis aries*), domestic cat (*Felis catus*) and domestic dog (*Canis familiaris*). ATMs of these species are granulated lysosome-rich cells with lamellipodial protrusions and express the lysosome markers acid phosphatase 5 (ACP-5) and Mac-3/Lamp-2. Using ACP-5 and Mac-3/Lamp-2 as markers, we additionally detected ATMs in other species, such as the domestic horse (*Equus ferus caballus*), wild boar (*Sus scrofa*) and red fox (*Vulpes vulpes*). Feline and canine ATMs also express the murine macrophage marker F4/80 antigen. In the lean condition, the alternative macrophage activation marker CD206 is expressed by feline and canine ATMs and arginase-1 by feline ATMs. Obesity is associated with interleukin-6 and interferon gamma expression and with overt tyrosine nitration in both feline and canine ATMs. This resembles the obesity-induced phenotype switch of murine and human ATMs. Thus, we show, for the first time, that the presence of ATMs is a general trait of mammals. The interaction between the adipose cells and SVF immune cells might be evolutionarily conserved among mammals.

Keywords Macrophages · Adipose tissue · Inflammation · Alternative activation · Metabolism · Mammals

This work was supported by the Institute for Comparative Molecular Endocrinology (Director Prof. Jan Tuckermann) of the University of Ulm and the State of Baden-Württemberg, Germany.

Electronic supplementary material The online version of this article (doi:10.1007/s00441-015-2253-1) contains supplementary material, which is available to authorized users.

✉ Tamás Röszer
tamas.roeszer@uni-ulm.de

[1] Institute for Comparative Molecular Endocrinology, University of Ulm, Ulm, Germany

[2] Massachusetts Institute of Technology, Cambridge, USA

[3] Laboratory of Pathology and Bacteriology, Veterinary Diagnostic Directorate, Debrecen, Hungary

[4] Frédéric Joliot-Curie National Institute of Radiobiology and Radiohygiene, Budapest, Hungary

[5] Department of Obstetrics and Reproduction, Faculty of Veterinary Science, Szent István University, Budapest, Hungary

Introduction

Adipose tissue is a major form of energy storage in the body of mammals. In addition to its metabolic role as a depot of lipids and lipid-soluble vitamins, it has steroidogenic activity and synthesizes hormones and paracrine mediators that control appetite, lipid and carbohydrate metabolism and reproduction (Cinti 2012). Moreover, adipose tissue is involved in immune surveillance (Grant and Dixit 2015; Zhang et al. 2015). This group of functions suggests that the adipose tissue depots act as an integrated metabolic, endocrine and immune organ of the body (Ferrante 2013; Galic et al. 2010; Rosen and Spiegelman 2014).

Despite adipose tissue having indispensable physiological roles, the hyperplasia and the hypertrophy of adipose tissue cause obesity, which is a health problem reaching pandemic proportions today (Rosen and Spiegelman 2014). Obesity can disrupt the endocrine and the immune functions of the adipose tissue and this impairment of adipose tissue physiology has been recognized as a major predisposing factor for insulin resistance, diabetes, atherosclerosis and cancer (Lee and Lee 2014).

The two cellular constituents of adipose tissue are the fat cells or adipocytes and the cells of the so-called stromal vascular fraction (SVF; Fig. 1). In rodents and primates, the SVF contains mesenchymal stem cells and various immune cells (Cinti 2012). The functions of the SVF cells are the subject of intensive research today, since they have the potential to impede obesity development and to resolve obesity-associated immune and metabolic dysfunctions (Chhabra and Brayman 2013; Paek et al. 2014). The stem cells of the SVF differentiate into mature adipocytes and thus, the inhibition of their differentiation program can be an approach against obesity (Rosen and Spiegelman 2014). Furthermore, the in vitro differentiation potential of the SVF stem cells makes them promising tools in tissue engineering, with potential use in regenerative medicine (Tsuji et al. 2014). The SVF immune cells, such as mast cells, regulatory T cells, granulocytes and adipose tissue macrophages (ATMs) have recently been recognized to affect metabolism through paracrine and endocrine mechanisms (Grant and Dixit 2015). Changes in the quantity and the nature of the SVF-associated immune cells can cause insulin resistance and diabetes (Osborn and Olefsky 2012). In this context, ATMs are the most intensively studied immune cells of the SVF. They have several functions in endocrine signaling by synthesizing hormones and

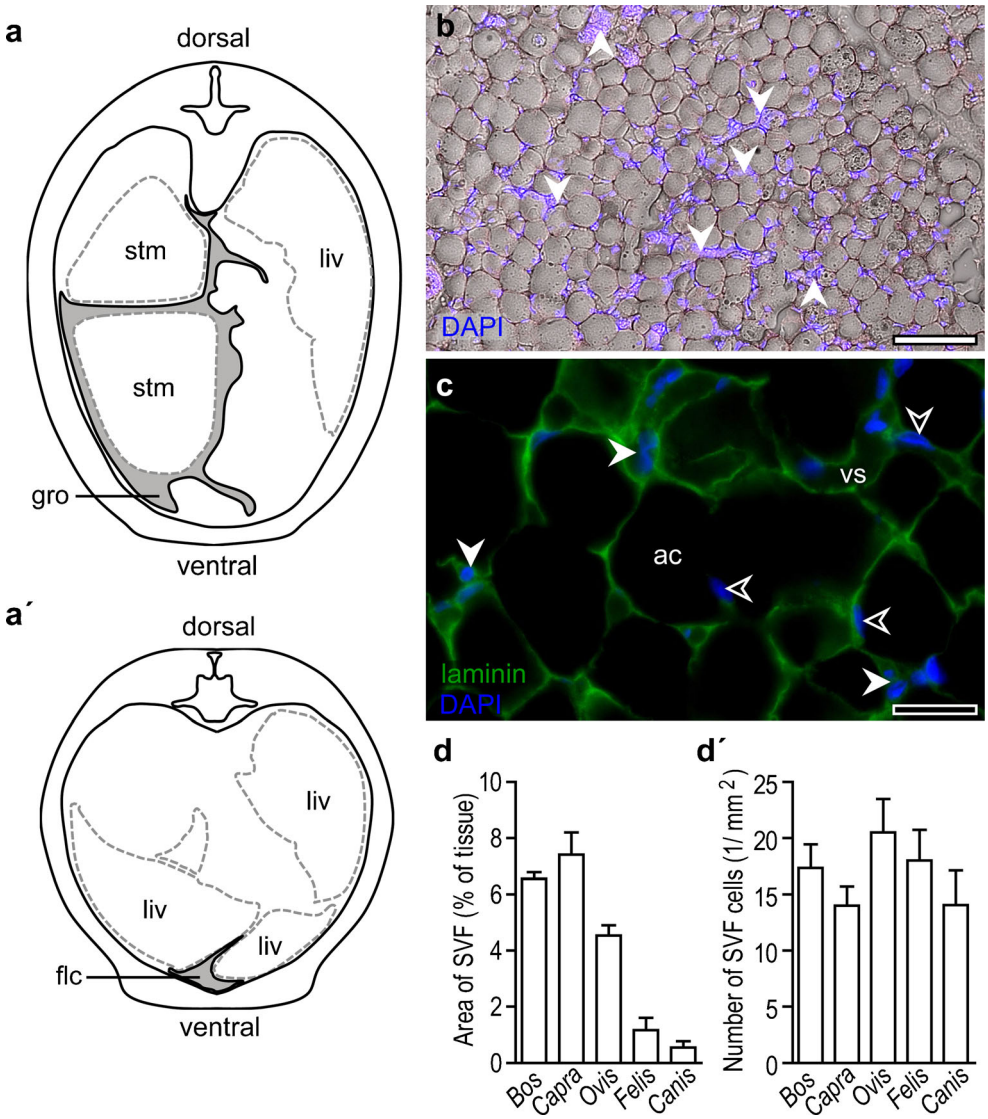

Fig. 1 Localization of fat depots and amount of stromal vascular fraction in the species studied. **a**, **a'** Localization of visceral fat depots analyzed in this study. **a** The greater omentum (*gro*) was the source of the fat samples in *Bos*, *Capra*, *Ovis* and *Felis*. **a'** Adipose tissue was collected from the falciform ligament (*flc*) in *Canis*. The schemes show the visceral fat localization in the abdominal region (*liv* liver, *stm* stomach). **b** Stromal vascular fraction (SVF) cells (*arrowheads*) surround adipose cells. Differential interference contrast image of canine adipose tissue. Cell nuclei were labeled with 4,6-diamidino-2-phenylindole (*DAPI*). *Bar* 150 μm. **c** Laminin immunostaining labels the extracellular matrix in which the adipose cells (*ac*) and SVF cells are embedded. Nuclei of the SVF cells (*closed arrowheads*) are localized in laminin-stained fields and allow them to be distinguished from the nuclei of the adipocytes (*open arrowheads*). *Bar* 50 μm. **d**, **d'** Area and cellularity, respectively, of the SVF as measured on adipose tissue sections

adipokines that enable interference with insulin-controlled metabolism (Epelman et al. 2014; Glass and Olefsky 2012; Lee and Lee 2014; Li et al. 2013; Osborn and Olefsky 2012; Qiu et al. 2014). The ATMs of the visceral adipose tissue, especially, have prime importance in metabolic regulation (Rosen and Spiegelman 2014). When ATMs are stimulated with bacterial cell-wall component lipopolysaccharides (LPS), interferon gamma (IFNγ), or modified lipoproteins, they adopt a so-called classical (or M1) activation state. The M1 activated ATMs produce inflammatory cytokines, nitric oxide (NO) and reactive oxygen species. These mediators inhibit insulin signaling locally and, by entering the bloodstream, cause systemic insulin resistance and exacerbate autoimmunity and pancreatic beta cell destruction (Fuentes et al. 2010; Glass and Olefsky 2012; Lee and Lee 2014; Osborn and Olefsky 2012). The M1 activation of the ATMs is thus a key mechanism in the development of the obesity-associated impairment of adipose tissue physiology. On the contrary, ATMs can also adopt an alternative (often called M2) activation state in response to cytokine signals from other immune cells of the SVF (Qiu et al. 2014) and possibly to various lipid metabolites, hormones and lipid soluble vitamins (Röszer et al. 2013; Zeyda et al. 2007). M2 activation is thought to support the homeostatic endocrine functions of the ATMs (Rosen and Spiegelman 2014), for instance, allowing ATMs increased adaptive thermogenesis (Qiu et al. 2014).

Collectively, the cells of the adipose tissue SVF have a high biomedical impact. However, the majority of the studies addressing the role of the SVF cells has been conducted in murine models of human diseases, in clinical studies, or in non-human primates (Chung et al. 2014; Greenberg and Obin 2006) and thus, we lack information on the nature and the functions of the SVF in other mammals. Only a negligible number of studies have been carried out on SVF stem cells (Marx et al. 2015) and we have no information on the immune phenotype of the SVF outside of rodents and primates. Therefore, whether the role of the SFV in metabolic regulation is a general trait of mammals is unknown. Interaction between immune cells and metabolically active tissues occurred at an early stage of evolution (Röszer 2014); however, the lack of comparative studies makes the evolutionary origin of the interaction between SVF immune cells and adipose cells uncertain.

We hypothesize that the immune function of the SVF is a general trait of mammals. This study is aimed at establishing this possibility by the analysis of the SVF composition in various mammals. We analyze farmed ruminant species, such as cattle (*Bos primigenius taurus*), domestic goat (*Capra aegagrus hircus*) and sheep (*Ovis aries*). In these animals, adipose tissue is important in the determination of meat and milk production and in the maintenance of fertility (Szebeni et al. 2007). We also study animals frequently brought to veterinary practices, such as the domestic cat (*Felis catus*) and the domestic dog (*Canis familiaris*). In these animals, obesity as a result of overnutrition can develop raising health issues and complications in the care of feline and canine patients (de Godoy and Swanson 2013). Moreover, canine obesity is a possible model of human obesity associated metabolic diseases (Ionut et al. 2010) but we lack information on the SVF contribution to metabolism in dogs. We also analyze the SVF cells of red fox (*Vulpes vulpes*), wild boar (*Sus scrofa*) and horse (*Equus ferus caballus*). The studied species represent the order of Artiodactyls, suborders of the Ruminantia and Suina, the order of Perissodactyla and two superfamilies of the order of Carnivora, thus allowing comparisons between evolutionary diverse groups of mammals. We analyze the morphology and cell markers of the SVF, with emphasis on the resident immune cells.

Materials and methods

Animals and tissue harvest

We obtained SVF cells from white adipose tissue samples collected from cattle (*Bos primigenius taurus*; breed Hungarian Simmental, intact females, aged 2 months, n=5); domestic goat (*Capra aegagrus hircus*; breed Sanental, intact males, aged 5–8 months, n=4); sheep (*Ovis aries*; breed Kamieniec, intact males, aged 4–5 months, n=5); domestic cat (*Felis catus*; European shorthair, intact females, aged 3–4 years, n=6); domestic dog (*Canis familiaris*; mongrel, intact females, aged 5–8 years, n=9). We also analyzed samples from the domestic horse (*Equus ferus caballus*; aged 5 and 7 years, n=2). The animals were bred as farmed or companion animals and were free of any pathologies. Cattle, sheep, goat and horse specimens were collected during necropsies performed as part of the health screening of farmed animals. We analyzed specimens from wild boar (*Sus scrofa*; adult, n=2) and red fox (*Vulpes vulpes*; adult, n=2) captured in the wild and sent for veterinary necropsy. The data of the analysis of the domestic horse, wild boar and fox samples are shown in the Electronic supplementary material of this article. Adipose tissue samples were isolated from the greater omentum and stored in 4 % paraformaldehyde. Canine and feline specimens were collected as biopsy samples during surgical interventions performed at veterinary clinics by isolating adipose tissue from the falciform ligament and the greater omentum, respectively. The body condition score (BCS) was used to cluster the feline (Bjornvad et al. 2011) and the canine (Müller et al. 2014) samples into normal and obese categories. Three cats and five dogs were normal (BCS5 for cats, BCS3 for dogs); three cats and four dogs were obese (BCS7 for cats and BCS5 for dogs). Body condition and clinical history, plus blood

glucose and insulin levels, were recorded for each animal. Blood samples were obtained from the cephalic vein and fasted glucose and insulin levels measured as described previously (Müller et al. 2014). Sample collections were approved by the local authorities and the owners of the animals. Throughout the study, we used mouse SVF cells as a reference of antibody specificity (Figs. S1, S3). Mouse SVF cells were isolated from the epididymal adipose tissue of 8-week-old C57Black/6 lean mice (n=5; Jackson Laboratories, USA) or mice kept on a high-fat diet for 8 weeks (n=5, 60 % calories from fat, diet formula of Research Diets, USA). Mice were kept at a specific pathogen-free animal facility under a 12-h/12-h dark/light cycle and were killed in a carbon dioxide chamber before sample collection. The collection of mouse tissues was approved by local authorities.

Isolation of SVF cells and flow cytometry

To separate the SVF from fat cells, we used a method developed previously for SVF isolation from murine adipose tissue (Weisberg et al. 2003). The adipose tissue samples were washed in phosphate-buffered saline (PBS) and chopped into pieces with a surgical blade. The tissue pieces were suspended in 10 ml digestion medium composed of 7 ml Hank solution (H9269, Sigma Aldrich), 3 ml of a 7.5 % bovine serum albumin (BSA) solution and 20 mg collagenase II (C6885, Sigma-Aldrich). The tissues were digested at 37 °C for 2 h with 100 rpm agitation. After the digestion, we allowed the separation of an upper phase containing adipocytes and released fat and then discarded this phase. The lower phase was passed through a 100-μm mesh cell strainer and centrifuged for 10 min at 1500 rpm at 4 °C. The pellet was collected and resuspended in selection medium consisting of 2 mM EDTA and 0.5 % BSA in PBS, pH 7.4. The cells were further used in flow cytometry and transmission electron microscopy. For flow cytometry analysis, the cell density was adjusted to 10^6 cell/ml. Light scattering parameters were recorded by a BD LSR flow cytometer, with the counting of 10,000 events in each sample. After excluding doublets, we generated plots showing the side scatter area (SSC-A) in the function of the forward scatter area (FSC-A).

Transmission electron microscopy and image analysis

The SVF cells were adjusted to a 10^6 cell/ml density and 100 μl of the cell suspension was added to conical tubes and fixed by adding 200 μl of a 1:5 mixture of 4 % paraformaldehyde and glutaraldehyde. After overnight fixation, the cells were centrifuged for 5 min and the pellet was processed for embedding and ultrathin sectioning as described previously (Röszer et al. 2011). The ultrathin sections were analyzed with a JEM Jeol transmission electron microscope. Granulation of the Type A cells was quantified by using a semi-automated segmentation approach based on active contours (Kass et al. 1988). Each granule on the transmission electron micrograph was labeled by clicking on a point belonging to the granule and the algorithm defined a smooth contouring element most likely corresponding to the granule border. This was made possible by the prominent edges and uniformity of the granule interior. The granule number per cell and the granule volume normalized to cell volume were calculated.

Histochemical and immunohistochemical staining and image analysis

Tissue samples were fixed in 4 % paraformaldehyde. Samples were processed for paraffin embedding or cyrosectioning. For paraffin embedding, the samples were dehydrated in a graded series of alcohol, cleared in xylene, embedded into wax and cut with microtome. Sections were cleared with xylene and rehydrated and acid phosphatase 5 (ACP-5) was visualized by using a leukocyte acid phosphatase staining kit (387A-1KT, Sigma-Aldrich) according to the manufacturer's protocol. As a positive control of the ACP-5 staining, we used mouse femur sections and mouse osteoclasts cultured in vitro (Fig. S4). The processing of the bone samples and the culture conditions of the osteoclasts were as described previously (Menendez-Gutierrez et al. 2015). Adipose tissue sections were also processed for standard hematoxylin and eosin staining. Sections of canine adipose tissue were stained with 0.1 % toluidine blue pH 1.5 for 10 min to allow the staining of glucose-aminoglycan rich granules of the leukocytes (Módis 1974). Specimens were analyzed with a Leica microscope, by using bright field illumination, differential interference contrast (DIC), or a polarizing filter (Fig. S5).

For cryosectioning, the samples were immersed in 20 % sucrose solution overnight, then placed into Surgipath Cryo-Gel (Leica Microsystems, 39475237) for the embedding of fat-rich tissues and frozen at −80 °C. Sections were cut with a Leica cryostat at a chamber temperature of −25 °C. Cryosectioned specimens were used for the immunostaining of the lysosome protein Mac-3/Lamp-2 or laminin, which is a marker of the extracellular matrix of adipose tissue (Mori et al. 2014). Sections were covered with 0.1 % Triton-X 100 containing PBS and then incubated with 2 % normal goat serum for 1 h. After being washed with PBS, the samples were incubated overnight with a rat antibody raised against mouse Mac-3/Lamp-2 (sc 19991, Santa Cruz) or laminin (ab11575, AbCam). The primary antibodies were visualized with rhodamine or fluorescein isothiocyanate (FITC)-conjugated goat anti-rabbit immunoglobulins (Sigma-Aldrich) and the nuclei were labeled with 4,6-diamidino-2-phenylindole (DAPI) by using Vectashield fluorescent mounting medium (Vector Laboratories). The sections were analyzed with a Leica

fluorescent microscope. As a negative control, we preformed immunostaining with the omission of the primary antibodies. The specificity of the laminin antibody was tested on cryosections of mouse intestinal mucosa (Fig. S4). Images were taken with DIC and with fluorescent illumination.

To determine the area of the SVF in tissue seticons, we used image analysis. Images were taken at 20× bright field magnification of sections stained with hematoxylin and eosin. In each image, a global threshold was computed by using Otsu's method (Kass et al. 1988). This was used to convert the gray level intensity image to binary images, whereby black pixels corresponded to the stromal fraction and white pixels corresponded to the fat cells. The percentage of black pixels in each image was then outputted and plotted. The SVF cell number was determined by DAPI nuclear staining on sections stained for laminin. Rounded cell nuclei in laminin-positive fields were counted as SVF cells, whereas cell nuclei attached to the contours of the fat cells were considered as adipocyte nuclei. Cell counts were normalized to the tissue area.

Fluorescence-assisted flow cytometric analysis of SVF cells

SVF cells were centrifuged for 5 min at 1500 rpm and the pellet was resuspended in red blood cell lysis buffer (Sigma Aldrich). After being washed with selection buffer, the cells were fixed with intracellular fixation buffer (00822240, Affymetrix eBioscience) and washed with selection buffer and the cell density was adjusted to 10^6 cells/ml. We used 200 μl of the cell suspensions. First, the cells were incubated with Fc receptor blocker (553141, BD Biosciences) for 1 h and then the isotype control immunoglobulins (rat phycoerythrin conjugated IgG2a, 12-4321-80, Affymetrix eBioscience; FITC-conjugated rat IgG, 406001, BioLegend; allophycocyanin-conjugated streptavidin, 47-4317-82, eBioscience; e-Fluor 450, 48-4321-80, eBioscience) or the specific antibodies. To label ATMs, we used antibodies directed against lysosome proteins ACP-5 and Mac-3/Lamp-2. The antibody specificity for ACP-5 and Mac-3/Lamp-2 was controlled by Western blotting (Fig. S3). For the preparation of cell lysates, tissues were homogenized in RIPA lysis buffer (150 mM NaCl, 20 mM TRIS pH 7.5, 1 % Nonidet P40, 5 mM EDTA). Lysates were centrifuged at 1500 rpm for 10 min and the protein concentration was measured in the supernatant colorimetrically. The solubilized proteins were separated by 10 % SDS-polyacrylamide gel electrophoresis. After transfer to nitrocellulose membrane (Bio-Rad, Germany), the membranes were blocked with 3 % bovine serum albumin for 1 h and then probed with the ACP-5 and the Mac-3/Lamp-2 antibodies for 18 h at 1:10,000 antibody dilution. Feline and canine SVF cells were also stained for mouse F4/80 antigen and macrophage activation markers arginase-1, CD206 and cytokines interleukin-6 (IL-6) and IFNγ. As a hallmark of ongoing NO synthesis (Röszer 2012), we labeled nitrosylated tyrosine. The following antibodies were used: phycoerythrin-conjugated anti-mouse Mac-3/Lamp-2 (553324, BD Pharmingen), allophycocyanin-conjugated anti-mouse F4/80 antigen (17-4801-80, Affymetrix eBioscience), FITC-conjugated anti-mouse CD206 (123005, BioLegend), FITC-conjugated anti-human arginase-1 (IC5868F, RD Systems), phycoerythrin-conjugated anti-mouse IL-6 (554401, BD Pharmingen), e-Fluor 450 (Pacific blue substituent)-conjugated anti-mouse IFNγ (48-7311-80, Affymetrix eBioscience) and unconjugated mouse anti-nitro tyrosine (SMC-154D, StressMarq). After a 2-h incubation, the cells were washed in selection buffer and used for analysis. The unconjugated nitro-tyrosine antibody was secondarily labeled with Alexa-488-conjugated goat anti-mouse antibody (A11008, Life Technologies) for 1 h. Acid phosphatase 5 (ACP-5) was labeled in a two-step indirect immunostaining method. The cell suspensions were treated with permeabilization buffer (00833356, eBioscience) and incubated with anti-mouse ACP-5 antibody overnight. After being washed in selection buffer, the cells were incubated with Alexa-488-conjugated goat anti-rabbit antibody (A11008, Life Technologies) for 1 h. Finally, the cells were washed with selection buffer and analyzed. We used a BD LSR flow cytometer for analysis. We counted 10,000 events. For data acquisition, we used FACSDiva (BD Biosciences) software and, for analysis, FlowJo (Tristar, USA) software.

Gene expression analysis

For quantitative polymerase chain reaction (qPCR) analysis, total RNA was isolated from SVF cells by using TRI Reagent (T9424, Sigma-Aldrich). Transcripts were quantified in a two-step reverese transcription qPCR process by using a Life Technologies ViiA7 qPCR instrument. We used the following primer pairs for amplification: *Emr1* (encoding F4/80 antigen) Fw CGTGTTGTTGGTGGCACTGTGA, Rv CCACATCA-GTGTTCCAGGAGAC; *Arg1* (encoding arginase-1) Fw CATTGGC-TTGCGAGACGTAGAC Rv GCTGAAGGTCTCTTCCATCACC; *Cd206* (encoding CD206) Fw CCACAGCATTGAGGAGTTTG, Rv ACAGCTCATCATTTGGCTCA; *Il6* (encoding IL-6) Fw GCTACCAAACTGGATATAATCAGGA Rv CCAGGTAGCTATGGTACTCCAGAA; *Ifng* (encoding IFNγ) Fw TAGCC-AAGACTGTGATTGCGG, Rv AGACATCTCCTCCCATCAGCAG. For normalization of the transcript levels, we used beta actin (Fw GCACCAGGGTGTGATGGTG, Rv CCAGATCTTCTCCATGTCGTCC).

Statistical analysis

Data are presented as means±standard deviation. Statistical significance of the difference between data of lean versus

obese canine and feline specimens was determined by the use of an unpaired two-tailed Student *t*-test.

Results

Morphology of SVF cells

General details of the SVF from the visceral adipose depots from *Bos*, *Capra*, *Ovis*, *Felis* and *Canis* are shown in Fig. 1a–c. As a reference, we used SVF isolated from the epididymal fat depots of 8-week-old C57Black/6 mice. In tissue sections, the area of the SVF was 6.55±0.23 % in *Bos*, 7.41±0.78 % in *Capra*, 4.53±0.36 % in *Ovis*, 1.16±0.44 % in *Felis* and 0.55±0.22 % in *Canis*, expressed as a percentage of the total tissue area (Fig. 1d). Based on the forward and side scatter areas (SSC-A and FSC-A, respectively), we could distinguish two cell populations in all species analyzed (Figs. 2a, S1). We refer to these cell populations as Type A and Type B. In mice, the Type A population contained cells expressing mouse macrophage markers F4/80 antigen and Mac-3/Lamp-2 (Fig. S1). This finding was in accordance with previous studies showing that this cell population is rich in ATMs (Morris et al. 2012). The Type B population was lacking F4/80 and Mac-3/Lamp-2 expression (Fig. S1). This accords with a previous finding that this cell population contains immature myeloid cells (Morris et al. 2012). In all species, the Type A population contained larger cells than the Type B population, as shown by their higher FSC-A values (Figs. 2a, S1). Cells of the Type A population had medium and high SSC-A values, which was indicative of intracellular granulation (Figs. 2a; S1). In all species, the Type A population was more abundant than the Type B (Fig. 2a').

Next, we analyzed the cell morphology of the SVF cells by transmission electron microscopy. We found two distinct cell types in all species studied. One cell type was lacking or had moderate intracellular granulation and had a centrally located and non-segmented nucleus (Fig. S2). These morphological features support the idea that these cells represent the Type B population in all species. The other cell type was larger in size, with the cytoplasm being filled with electrolucent vesicles or granules and had a segmented nucleus (Fig. 2b–h). This cell type represented the Type A cell population and in *Bos*, *Capra*, *Ovis* and *Felis* had electrolucent clear vesicles (Fig. 2c–e'). Based on their morphological features, we classified these vesicles as primary lysosomes. The Type A cells often also contained large vesicles that were moderately electrodense (Fig. 2b, e'). These structures were considered as phagosomes or secondary lysosomes. Invaginating cell membrane structures were also often recognized on Type A cells, suggesting that these cells were undergoing endocytosis activity (Fig. 2c, e–g). These cells contained few mitochondria, which suggests that these cells were non-activated resident immune cells (Ghernati et al. 2000). The Type A cells also had lamellipodial protrusions (Fig. 2e, g), characteristic features of tissue-resident macrophages (Rodrigues et al. 2010).

In *Canis*, the Type A cells displayed a heterogeneous morphology. Cells bearing lamellipodial protrusions, clear electrolucent vesicles and small amounts of electrodense granules were present (Fig. 2g). We also found cells in which the electrodense cytoplasmic granules were more abundant than the electrolucent granules (Fig. 2h).

Acid phosphatase 5 is present in adipose tissue macrophages

Next, we aimed to verify that the Type A cells were resident ATMs. Lysosomes are prevalent cell organelles of macrophages because of their phagocytosis activity and thus, we decided to label lysosome proteins. Lysosomes contain acid phosphatases (Pavelka and Roth 2010). Therefore, as a first approach regarding lysosome labeling, we detected acid phosphatase 5 (ACP-5) by using enzyme histochemistry (Janckila et al. 2007; Fig. S4). The ACP-5 activity was detected in scattered SVF cells in all species analyzed (Fig. 3a–e) and was confined to lysosome-like cytoplasmic granules. When we probed the isolated SVFs for ACP-5 by using an antibody raised against mouse ACP-5, we found that it was present in Type A cells and was lacking in Type B cells (Fig. 3f). Western blotting of the SVF cell lysates confirmed that the used ACP-5 antibody labeled an identical molecular weight protein band in all of these species (Fig. S3).

The majority of the Type A cells was classified as ACP-5-positive Type A in *Bos*, *Capra*, *Ovis* and *Felis* (68±7, 58±4, 78±6 and 56±9 %, respectively). ACP-5-negative Type A cells were prevalent in *Canis* (47±8 %). This accords with our ultrastructural observations showing that the canine SVF had a heterogeneous cell population with variable cytoplasmic granulation. The intracellular vesicle content of the Type A cells in *Bos*, *Capra*, *Ovis* and *Felis* was likely formed by lysosomes and endosomes, which were electrolucent by transmission electron microscopy and contained ACP-5. In *Canis* Type A cells, lysosomes were accompanied by electrodense cytoplasmic granules. Electrodense granules in canine leukocytes have been identified by others as lysosomes (Ghernati et al. 2000), lipid droplets, neutrophil, or eosinophil granules (Baldwin and Becker 1993).

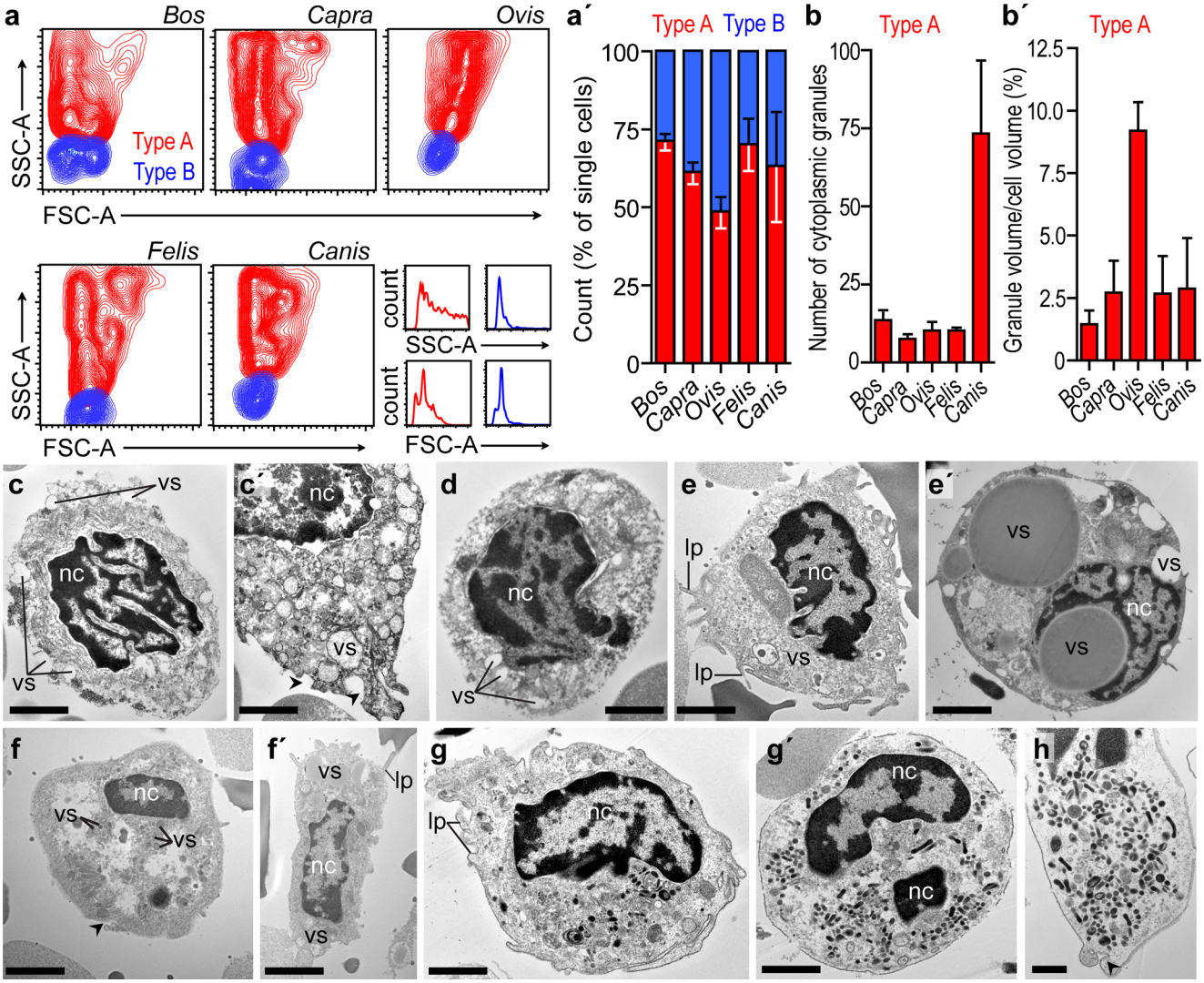

Fig. 2 Cell composition of the stromal vascular fraction (SVF). **a** Flow cytometry (FACS) analysis of single cells from the SVF. Representative plots show the side scatter area (SSC-A) and the forward scatter area (FSC-A) for each species studied. The distribution of SVF cells with various SSC-A and FSC-A values in *Canis* is given in the histograms *bottom right*. **a'** Graph summarizing the percentage of the Type A (*red*) and the Type B (*blue*) cell population in the SVF. Data were determined by using three samples obtained from each species. **b**, **b'** Image analysis of the Type A cells. Number of granules per cell (**b**) and the volume of the granules per total cell volume (**b'**). **c–h** Transmission electron microscopy analysis of Type A SVF cells of each species studied (*vs* clear electrolucent vesicles, *nc* nucleus, *lp* lamellipodia, *arrowheads* endosome formation) : *Bos* (**c**, **c'**), *Capra* (**d**), *Felis* (**e**, **e'**), *Ovis* (**f**, **f'**), and *Canis* (**g**, **g'**, **h**). *Bars* 5 μm (**c**, **d**, **e**, **e'**, **f**, **f'**, **g**, **g'**), 2 μm (**c'**, **h**)

By toluidine blue staining, we could detect birefringent granules in the *Canis* SVF cells (Fig. S5), resembling the staining pattern of mast cells (Módis 1974). This showed that the large SVF cells contained glycosaminoglycan-rich granules in *Canis*.

Mac-3/Lamp-2 is a general marker of adipose tissue macrophages in non-rodent mammals

Major types of murine macrophages express Mac-3, also known as lysosomal-associated membrane protein 2 (Lamp-2, CD107b; Flotte et al. 1983). Mac-3/Lamp-2 is a 110-kDa type I membrane glycoprotein and is expressed on lysosomal membranes and the plasma membrane (Huynh et al. 2007). The Type A cells isolated from the mouse SVF showed intensive staining for Mac-3/Lamp-2 (Fig. S1). Homolog genes of *Lamp2* have been found in the species that we tested in this study: *Bos taurus*, Gene ID: 529148; *Capra hircus*, Gene ID: 102189841; *Ovis aries*, Gene ID: 101113307; *Felis catus*, Gene ID: 100169945; *Canis lupus familiaris*, Gene ID: 481037. In order to test whether ATMs expressed Mac-3/Lamp-2 in these species, we probed adipose tissue sections (Fig. 4a–f) and isolated SVF cells (Fig. 4g) for Mac-3/Lamp-2 expression. We used antibodies raised against mouse Mac-3/Lamp-2. In all tested species, we found Mac-3/Lamp-2-expressing SVF cells scattered among adipose cells (Fig. 4a–

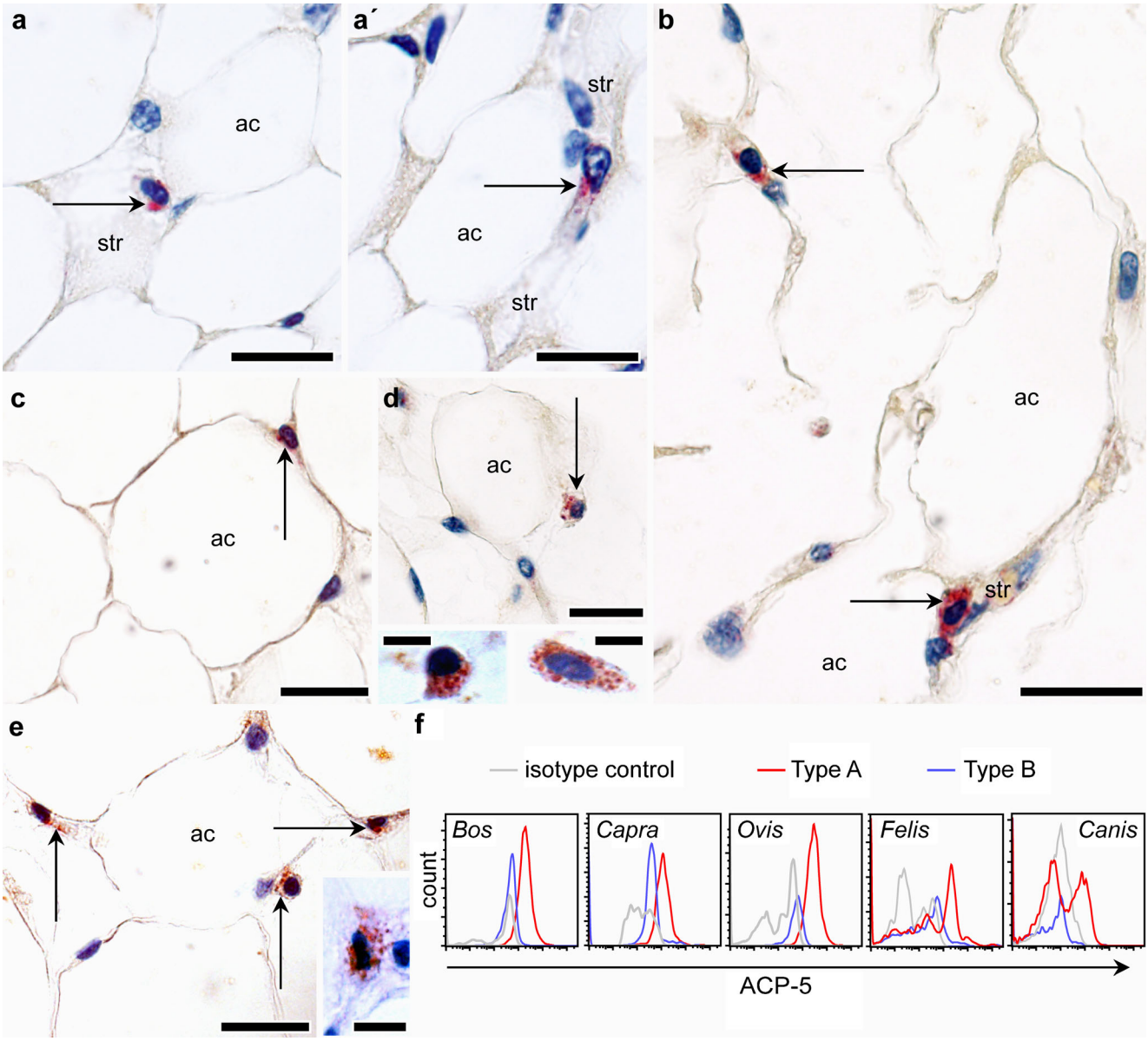

Fig. 3 Acid phosphatase 5 (*ACP-5*) expression by resident ATMs. **a–e** Enzyme histochemistry for ACP-5 in white adipose tissue from *Bos* (**a**, **a'**), *Capra* (**b**), *Felis* (**c**), *Canis* (**d**) and *Ovis* (**e**). *Arrows* indicate ACP5-containing cytoplasmic granules (*ac* adipocyte, *str* stroma). *Bars* 50 μm (**a–e**), 25 μm (*inserts* in **d**, **e**). **f** Representative histograms obtained by FACS analysis of the SVF cells (*gray line* fluorescence intensity of cells incubated with isotype control immunoglobulins, *red line* fluorescence intensity of Type A cells after staining with ACP-5 antibody, *blue line* fluorescence intensity of Type B cells after staining with ACP-5 antibody)

e). The staining was confined to cytoplasmic granules (Fig. 4f), suggesting that Mac-3/Lamp-2 was associated with lysosomes. The isolated SVF cells also expressed Mac-3/Lamp-2 and the expression was confined to the Type A population (Fig. 4g). By Western blotting of the SVF cells, we could detect the identical molecular weight bands in the tested species (Fig. S3).

Taken together, these findings confirm that the Type A cells represented ATMs in *Bos*, *Capra*, *Ovis*, *Felis* and *Canis* and that these cells expressed ACP-5 and Mac-3/Lamp-2. To test whether, by using these markers, ATMs can be detected in other mammals, we analyzed adipose tissue samples of wild

Fig. 4 Distribution of Mac-3/Lamp-2 in white adipose tissue. ▶ Cryosections of white adipose were labeled with an antibody raised against mouse Mac-3/Lamp-2. **a–e** Differential interference contrast (DIC) images. **a'–e'** Fluorescence illumination of the same sections. *Bos* (**a**, **a'**), *Capra* (**b**, **b'**), *Ovis* (**c**, **c'**), *Felis* (**d**, **d'**) and *Canis* (**e**, **e'**). *Bars* 250 μm. **f** *Canis* white adipose tissue with merged channels of the DIC and fluorescence illumination (*red* Mac-3/Lamp-2-containing cytoplasmic granules, *blue* cell nuclei stained with DAPI, *ac* adipocyte). *Bar* 50 μm. **g** FACS analysis of the SVF cells. Representative histograms showing the fluorescence intensity of the isotype control (*gray*) and the Type A cells labeled with Mac-3/Lamp-2 antibody (*red*)

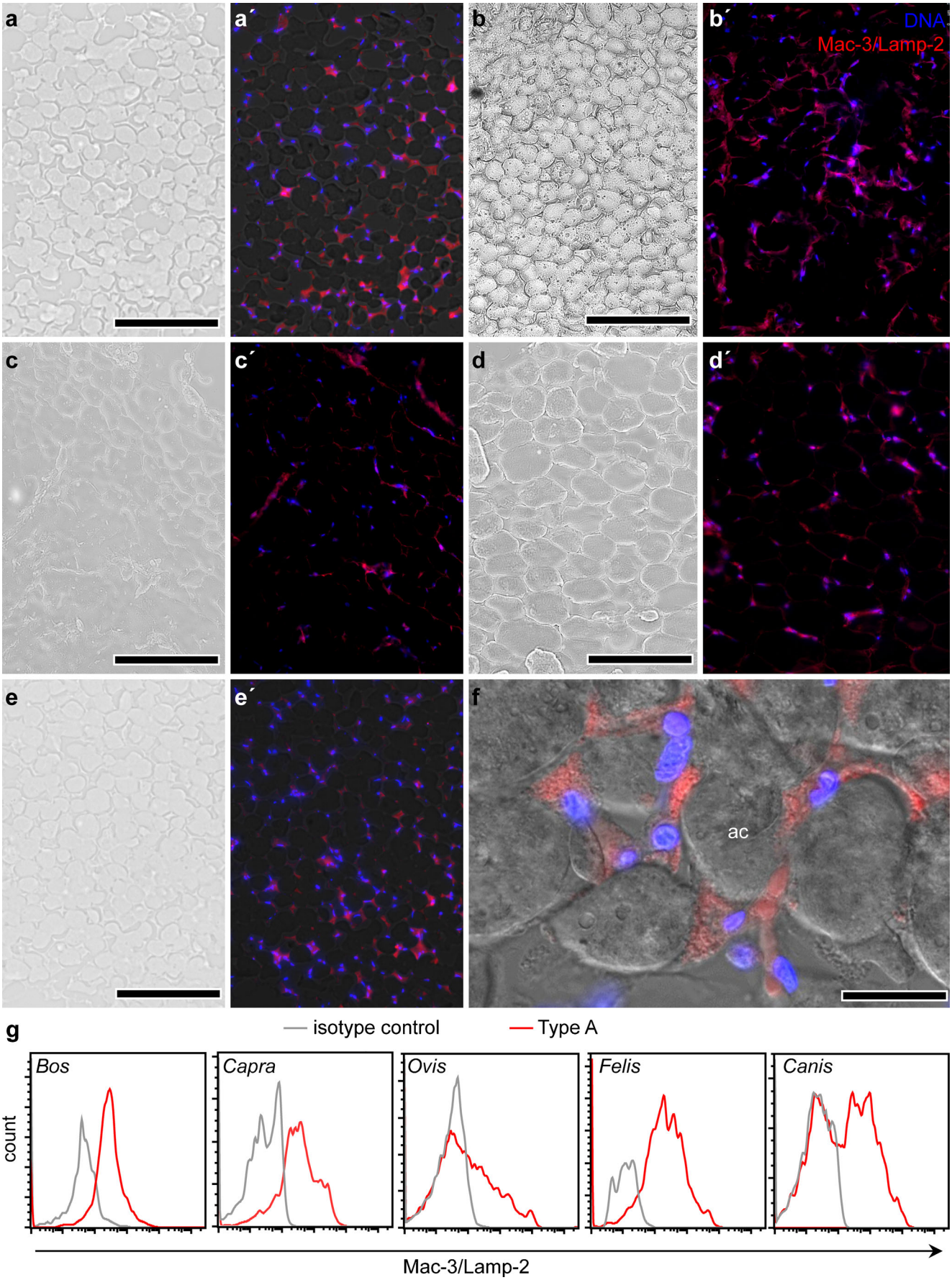
a
a´
b
b´
DNA
Mac-3/Lamp-2
c
c´
d
d´
e
e´
f
ac
g
isotype control
Type A
Bos
Capra
Ovis
Felis
Canis
count
Mac-3/Lamp-2

boar (*Sus scrofa*), red fox (*Vulpes vulpes*) and domestic horse (*Equus ferus caballus*; Figs. S6–S9). We could distinguish Type A and Type B cell types in the SVF of these species. We also found that the Type A cells expressed Mac-3/Lamp-2 and ACP-5 (Fig. S6). The Mac-3/Lamp-2- and ACP-5-positive SVF cells were scattered among the adipocytes, showing the distribution pattern of ATMs (Fig. S7–S9).

Immune phenotype of resident feline and canine ATMs

An intriguing question is whether the nutritional state has an effect on the immune phenotype of the ATMs in mammals other than rodents and primates. Overnutrition and an eventual positive energy balance is a common problem in dogs and cats kept in urbanized societies as companion animals (de Godoy and Swanson 2013). Thus, we continued our study with an analysis of tissue samples taken from visceral adipose tissue of lean and obese age- and gender-matched feline and canine individuals.

First, we tested whether the resident feline and canine ATMs (Type A cells) expressed similar markers to those of mouse resident ATMs. We probed the SVF cells for the expression of the F4/80 antigen, also known as EMR1 (egf-like module containing, mucin-like, hormone receptor-like 1). The F4/80 antigen is the product of the *Emr1* gene, which is a member of the EGF-TM7 family of leukocyte plasma membrane heptahelical molecules (Gordon et al. 2011). It is commonly expressed by mouse monocytes and many but not all types of tissue macrophages, including ATMs (Gordon et al. 2011). Homologs of the *Emr1* gene have been found in many mammalian species, including *Felis catus* (Gene ID: 100174782) and *Canis lupus familiaris* (Gene ID: 485015). Thus, we tested whether the resident feline and canine ATMs could be recognized by an antibody raised against the mouse F4/80 antigen. As we expected, the mouse visceral adipose tissue contained an F4/80-expressing ATM population (Fig. S1). We could also detect *Emr1* transcription and F4/80 expression in the SVF from *Felis* and *Canis* (Fig. 5a, a').

The immune phenotype (M2 versus M1 activation state) of the resident ATMs is a key factor in the metabolic impact of the ATMs (Lumeng et al. 2007). Thus, we next assessed whether the feline and the canine ATMs expressed markers of mouse M2 macrophage activation. First, we labeled the SVFs with an antibody raised against mouse CD206, a widely used marker of the M2 activation state in mice (Murray et al. 2014; Röszer 2015). *Cd206* transcription and CD206 protein expression was seen in the SVF of both *Felis* and *Canis* (Fig. 5b, b'). Next, we labeled the SVF cells with an antibody reacting with arginase-1, an enzyme assigned to the M2 activation state (Murray et al. 2014). *Arg1* transcription was detected in *Felis* and was negligible in *Canis* SVF (Fig. 5c). Accordingly, arginase-1 expression was found only in the feline ATMs (Fig. 5c'). Transcription of M1 activation markers *Il6* and *Ifng* was not detectable in the lean condition (Fig. S10).

Obesity and immune phenotype of feline and canine ATMs

Next, we analyzed SVF cells from obese feline and canine adipose tissue. The fasting blood glucose level was 5.67± 0.88 mM in lean cats and 11.13±4.3 mM in obese cats (P= 0.27). In dogs, the fasting blood glucose level was 4.23± 0.13 mM in the lean condition and 5.37±0.20 mM in obesity (P<0.05), with corresponsing plasma insulin levels at 3.43± 0.60 and 2.39±0.56 mU/l, respectively (P=0.26).

In both feline and canine obesity, we found *Il6* and *Ifng* transcription in the SVF cells (Fig. S10). In FACS analysis, the SVF cells were labeled with antibodies raised against mouse IL-6, mouse IFNγ and nitro-tyrosine (Fig. 6). Expression of IL-6 and IFNγ and increased tyrosine nitration attributable to the increased expression of inducible nitric oxide synthase (NOS2) are associated with M1 macrophage activation (Murray et al. 2014). The M1 activation of ATMs is a cause of insulin resistance in obese mice and human patients (Glass and Olefsky 2012).

In the lean condition, the feline ATMs failed to express IL-6 and lacked tyrosine nitration (Fig. 6a, a'). However, a low number of feline ATMs expressed IFNγ in the lean condition (Fig. 6a''). Interestingly, a low percentage of the circulating monocytes was also IFNγ-positive in feline blood but not in canine blood (Fig. S11). Feline obesity resulted in a marked increase of IL-6- and IFNγ-positive ATMs and caused tyrosine nitration (Fig. 6a–a''). In ATMs isolated from mice fed a high-fat diet, tyrosine nitration of the ATMs was associated with the expression of NOS2 (Fig. S1). Canine ATMs lacked IL-6 and IFNγ expression in the lean condition (Fig. 6c, c''); however a low percentage of the ATMs contained nitro-tyrosine (Fig. 6c'). Canine obesity led to IL-6 and IFNγ expression by ATMs, together with their increased tyrosine nitration (Fig. 6c–c''), indicating M1-like activation.

In mice and humans, not only the M1 activation of the resident ATMs but also the recruitment of inflammatory monocytes and the local proliferation of ATMs can contribute to adipose tissue inflammation (Amano et al. 2014; Rosen and Spiegelman 2014). In order to test whether the number of ATMs was increased in feline and canine obesity, we considered the number and distribution of ATMs in the adipose tissue. In feline obesity, the inflammatory phenotype switch of the ATMs was not associated with an increase of ATM

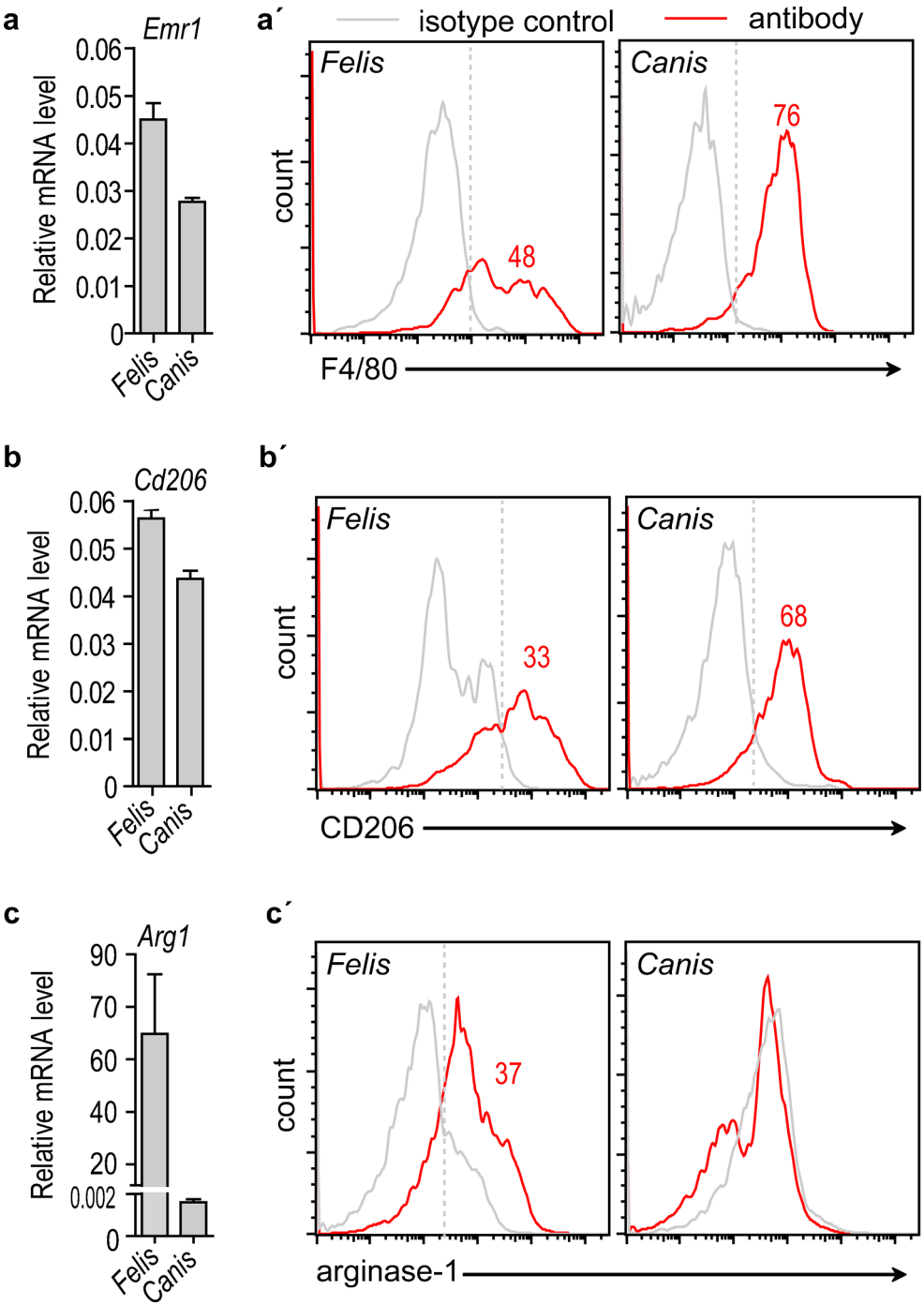

Fig. 5 Phenotype of ATMs in lean feline and canine adipose tissue. We assessed the expression of F4/80 antigen (**a**), CD206 (**b**) and arginase-1 (**c**) in lean feline and canine SVF. The mRNA transcript levels of *Emr1* (encoding F4/80 antigen), *Cd206* (encoding CD206) and *Arg1* (encoding arginase-1) were measured by quantitative polymerase chain reaction in SVF cells pooled from three samples. Transcript levels were normalized to the transcript level of beta actin (**a**–**c**). With FACS analysis of the SVF cells (**a'**–**c'**), we assessed the expression of F4/80, CD206 and arginase-1 in ATMs (Type A SVF cells). *Red lines* indicate the fluorescence intensity of ATMs labeled with antibodies raised against F4/80 antigen, CD206 and arginase-1. Isotype controls are shown in *gray*. The percentage of the positive cell populations is indicated

number (Fig. 6b). The adipose tissue contained 1.3±0.5 million/g tissue Type A cells in the lean condition and 1.1±0.4 million/g in obesity. The number of ACP-5-positive ATMs was 6.2±2/field in lean adipose tissue and 7±1.2/field in obesity. However, in canine obesity, a marked increase of the ATM number was observed. In the lean condition, the SVF contained 1.5±0.6 million/g tissue Type A cells. This cell density was raised to 3.25 ±0.9 million/g tissue in obesity ($P<0.01$). By using acid toluidine blue staining and ACP-5 histochemistry, we also compared the distribution of the birefringent and ACP-5-positive ATMs in lean and obese conditions (Fig. 6d). The mean cell count was 2.1±0.4 cells/field in the lean condition and 6.2±0.9 in obesity ($P<0.01$).

Discussion

Comprehension of SVF cell functions in murine models of obesity and diabetes has advanced recently with the use of

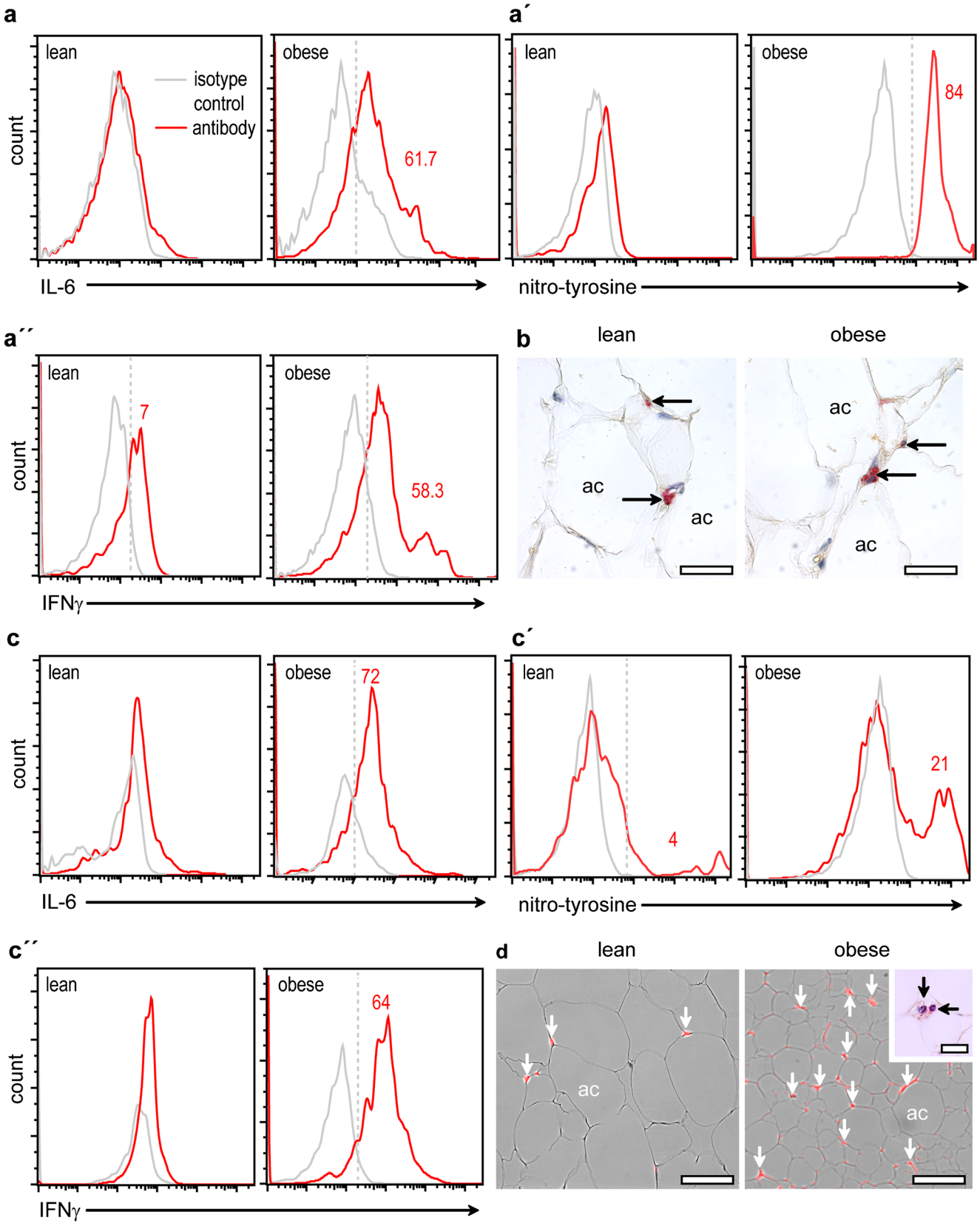
a
lean
obese
isotype
control
antibody
count
61.7
IL-6
a´
lean
obese
84
nitro-tyrosine
a´´
lean
obese
7
58.3
IFNγ
b
lean
obese
ac
ac
ac
ac
c
lean
obese
72
IL-6
c´
lean
obese
4
21
nitro-tyrosine
c´´
lean
obese
64
IFNγ
d
lean
obese
ac
ac

◀ **Fig. 6** Phenotype of the ATMs in obese feline and canine adipose tissue. **a–a"** FACS analysis of feline ATMs labeled with antibodies raised against interleukin-6 (*IL-6*), interferon gamma (*IFNγ*) and nitro-tyrosine. Isotype controls are shown in *gray*. The percentage of the positive cell populations is indicated. **b** ACP-5 histcochemical staining of lean and obese feline adipose tissue (*arrows* ATMs, *ac* adipocyte). *Bars* 25 μm. **c–c"** FACS analysis of canine ATMs labeled with antibodies raised against IL-6, IFNγ and nitro-tyrosine. Isotype controls are shown in *gray*. The percentage of the positive cell populations is indicated. **d** Birefringent ATMs in the white adipose tissue of lean or obese dog (*ac* adipocyte). *Insert* ACP-5-expressing ATMs. *Bars* 50 μm

gene targeting and transgenic approaches. In particular, the contribution of ATMs to insulin resistance and its associated pathologies has been studied extensively (Glass and Olefsky 2012; Grant and Dixit 2015). These studies promoted the understanding of specific gene functions in mouse ATMs and the discovery of the interaction of the immune system with the endocrine control of metabolism. Mice and humans share a large number of conserved genes in immunity and metabolism; this implies similar functions in the two species. However, key features of mouse and human ATMs, such as the molecular signature of their M1 and M2 activation and their relative proportions in obesity, exhibit differences (Shaul et al. 2010; West 2009). They raise the question as to whether the findings obtained in mouse studies can be directly extrapolated to other mammalian species. Despite the finding that inflammation can also lead to metabolic impairment in other mammalian species (Basinska et al. 2015), only a limited number of comparative studies of non-human primates and canines has explored the metabolic impact of adipose tissue inflammation (Chung et al. 2014; Castro et al. 2015; Bastien et al. 2015). Thus, whether adipose tissue hosts immune cells in mammals other than rodents and primates and whether these immune cells have the ability to regulate metabolism remains elusive. This investigation has partially filled this gap in our knowledge, showing that immune cells and specifically ATMs, are present in the adipose tissue in various mammalian species.

Our study shows that the SVF is rich in immune cells displaying characteristics of tissue-resident macrophages and monocytes in all the species tested. These immune cells lack similarities to dendritic cells (Ibisch et al. 2005; Mielcarek et al. 2007) or inflammatory leukocytes (Williamson and Grisham 1961). Based on their morphology and the expression of macrophage marker proteins ACP-5 and Mac-3/Lamp-2, we identified these cells as ATMs. The resident ATMs are major constituents of the SVF in all the tested species. Interestingly, the canine ATMs contain birefringent granules, which are electrodense when observed by transmission electron microscopy. Birefringent granulation is generally considered a hallmark of mast cells in dogs in which mast cells play a more prominent role in inflammatory and tissue healing processes than in other mammals (Dewald et al. 2004; Pucheu-Haston et al. 2015). This calls for caution when canine adipose tissue samples are analyzed by using acid toluidine blue, a standard staining method for mast cells, since ATMs are positively stained.

In ruminants, equine, feline and canine species, we have limited information on the cell markers of the tissue-resident macrophages (Yamate et al. 2000). Our study provides markers for the identification of ATMs in non-rodent mammals. We have shown that ACP-5 and Mac-3/Lamp-2 are general markers of ATMs in mammals. In some of the specimens, Mac-3/Lamp-2 expression has also been detected in endothelial cells (Fig. S8), calling for caution of the interpretation of the staining in the vicinity of blood vessels. Previous studies have shown that the family of Lamp-2 proteins is conserved from birds to mammals and that the diversity of Lamp-2 proteins is generated by alternative splicing of a single gene (Gough et al. 1995). This accords with our finding that Mac-3/Lamp-2 expression is detectable in all the species studied with antibodies raised against the mouse protein. This is possibly attributable to the presence of conserved epitopes in the tested species. The same stands for ACP-5. In humans, ACP-5 has been shown to be expressed by various macrophage populations (Janckila et al. 2007). As an aternative of immunostaining, ACP-5 enzyme histochemistry can also be used to label and further characterize the ATMs in various mammalian species. We also show that, in veterinary practice, feline and canine ATMs can be recognized by using the F4/80 antigen as a marker. This allows the flow cytometry analysis of ATMs isolated from biopsy samples and can expand the possible tools for studying ATMs in the context of metabolic diseases. Since obesity and diabetes is frequent in feline and canine patients at veterinary clinics (Müller et al. 2014), the further study of ATMs in these species might be a novel path by which to study the metabolic regulatory role of ATMs in non-rodent mammals.

In resident ATMs, we were able to detect protein cross-reacting with anti-mouse CD206 antibody in *Felis* and *Canis*. CD206, also termed MRC1 (C-type mannose receptor 1), is a 175-kDa type I transmembrane glycoprotein that binds and internalizes glycoproteins and collagen ligands (Porcheray et al. 2005). Several types of tissue-resident macrophages express CD206 in the mouse and the human, including ATMs (Aron-Wisnewsky et al. 2009; Dupasquier et al. 2006; Haase et al. 2014; Svensson-Arvelund et al. 2015; Titos et al. 2011; Zeyda et al. 2007). The immune functions of CD206 are not yet fully understood; for instance, its absence increases the random migration of macrophages and results in the up-regulation of proinflammatory cytokine production in the mouse (Kambara et al. 2015). The lack of CD206 also results in the elevated serum level of inflammatory proteins, suggesting that it has a role in the resolution of inflammation by clearing inflammatory molecules from the blood (Lee et al.

2002). Its gene transcription is amplified in macrophages undergoing M2 activation, in macrophages with profibrotic effects, or in macrophages that undergo a fibrocyte-like phenotype switch (Bellon et al. 2011; Kaku et al. 2014; Medbury et al. 2013). The CD206-encoding gene is conserved from birds to mammals (Staines et al. 2014); however, we have little information on the macrophage expression of CD206 outside of rodents. Equine myeloid cells express CD206 (Steinbach et al. 2005) and dog CD206 expression (Gene ID: 487114) has been reported in in vitro differentiated macrophages and in bone-marrow-derived dendritic cells (Ricklin Gutzwiller et al. 2010). One excretory product of the canine parasite *Toxocara canis*, which helps evade host defense and allows survival in the tissues, has a sequence similarity to CD206 (Loukas et al. 2000). However, the exact immune functions of CD206 are unknown in non-murine species. In the domestic cat, the CD206 gene sequence is known (Gene ID: 101092193) but its association with immune cells has not been studied as yet. This is the first study showing the in vivo steady-state transcription of *Cd206* and the expression of CD206 by tissue-resident macrophages in non-rodent mammals.

In *Felis* resident ATMs, we also found the transcription of *Arg1*, together with arginase-1 immunostaining. Arginase-1 is an enzyme of the urea cycle; it uses the amino acid L-arginine as a substrate and produces L-ornithine and urea. Furthermore, it is constitutively expressed by tissue-resident macrophages and its gene transcription is amplified in M2 activation in the mouse (Ahn et al. 2012; Dzik 2014). L-ornithine might be used in polyamine and collagen synthesis, promoting fibrosis and tissue regeneration (Munder 2009). The consumption of L-arginine by arginase-1 can inhibit L-arginine-dependent immune functions (Munder et al. 2006), such as the suppression of T-cell proliferation or oxidative NO synthesis (Munder et al. 1999; Röszer 2015).

Both CD206 and arginase-1 are markers of M2 macrophage activation in mice (Röszer 2015). However, whether the M1/M2 model of macrophage activation can be extrapolated to other mammals is unclear. M2 macrophage activation occurs as part of the so-called Th2 immune response in helminth infections and in the allergic response in mice (Murray et al. 2014). Helminth infections in dogs, cats and mice evoke distinct immune responses (de Almeida Leal et al. 2014) and each species has specific immune features in response to helminths or allergens (Dillon et al. 2008; Taglinger et al. 2007). In the feline allergic response, a clear Th2 immune response is lacking (Taglinger et al. 2008). In dogs, the Th2 immune response is present in allergic responses; however, whether this evokes M2 macrophage activation is uncertain. Nevertheless, canine macrophages in allergic reactions are low IFNγ producers and synthesize IL-4 (Fujiwara et al. 2003); this makes them similar to mouse M2 macrophages. Moreover, the blunted inflammatory activation of canine macrophages in response to adenosine and ATP (Fujimoto et al. 2012) and the increased prostaglandin production in response to ω-3 fatty acids (Kearns et al. 1999) resemble features of mouse M2 macrophages.

In *Felis*, the ATM number is not increased in obesity, despite ATMs displaying increased IL-6, IFNγ expression and tyrosine nitration compared with the lean condition. Interestingly, in the lean condition, a low number of ATMs express IFNγ, similar to blood monocytes. Feline monocytes have been previously shown consitutively to express cytokines (Kipar et al. 2005), including IFNγ (Van de Velde et al. 2013). Obesity increases both IL-6 and IFNγ transcription in feline adipose tissue (Van de Velde et al. 2013) and IFNγ might be a signal of macrophage activation in cats (Berg et al. 2005). The macrophage synthesis of NO has also been shown in cats (Ponti et al. 2001). Taken together, these data suggest that feline ATMs have steady-state IFNγ transcription and that obesity causes increased IL-6 and IFNγ expression and NO synthesis.

Similarly, canine obesity is associated with an inflammatory immune phenotype of the ATMs. In contrast to cats, the ATM number increases with obesity in dogs. We found increased numbers of ATMs expressing IL-6 and IFNγ, together with increased tyrosine nitration. As has been emphasized above, the immune and metabolic impact of ATMs has been most characterized in mouse models of human obesity, showing that ATMs produce these inflammatory mediators in obesity and that this is a causative of insulin resistance (Glass and Olefsky 2012). In mouse and in human macrophages, IL-6 and IFNγ gene transcription is upregulated through nuclear factor kappa beta (NFκB). We have no information as to whether a similar mechanism exists in feline and canine macrophages. However, in the canine macrophage cell line DH82, lipopolysaccharide treatment has been shown to induce inflammatory activation through NFκB (Kim et al. 2006). Lipopolysaccharides induce the expression of IL-6 in canine macrophages, such as DH82 cells (Fujimoto et al. 2012), blood mononuclear cells and Kupffer cells in vitro (Hamano et al. 2002; Shi et al. 1995). Moreover, IL-6 expression is associated with inflammation (Spitzbarth et al. 2011) and macrophage infiltration into inflamed tissues in dog (Klocke et al. 2005). IFNγ expression is also a result of the activation of blood mononuclear cells in the dog (Panaro et al. 2001) and increases the cytotoxic activity of canine alveolar macrophages in vitro (Kurzman et al. 1999). Monocyte-derived canine macrophages secrete IFNγ when they kill the intracellular parasite *Leishmania* (Turchetti et al. 2015). Taken together, these findings support the notion that the increased IL-6 and IFNγ expression of canine ATMs resembles the obesity-induced M1 macrophage activation in mice. However, whereas mouse M1

macrophages are high NO producers, conflicting results have been obtained regarding whether canine macrophages have a NO burst when they fight pathogens (Sanches et al. 2014). Our data also suggest that NO synthesis is associated with a subpopulation of canine ATMs in obesity.

The reason that the ATMs adopt an inflammatory phenotype in obesity in cats and dogs is intriguing. In mice and humans, the excess lipid storage by the adipose cells is a major contributor to the development of adipose tissue inflammation, monocyte recruitment to the adipose tissue and M1 activation of the ATMs (Glass and Olefsky 2012; Rosen and Spiegelman 2014). However, whether a similar mechanism exists in cats and dogs is unclear. Obesity causes adipose tissue inflammation in cats (Van de Velde et al. 2013); however, a high-fat diet increases oxidative stress rather than inflammation in the adipose tissue in cats (Verbrugghe et al. 2014). In dogs, lipid metabolites and liposomes increase inflammation (Szebeni et al. 2007) and weight loss improves the inflammatory state (Bastien et al. 2015). These findings suggest that lipid overload shifts ATMs into an inflammatory phenotype and that visceral obesity causes inflammation in dogs. Adipose tissue inflammation predisposes insulin resistance in mice and humans (Rosen and Spiegelman 2014); however, recent studies provide conflicting conclusions in dogs. A correlation between diabetes mellitus and serum levels of IL-6 has been shown in dogs (Kim et al. 2015) and the reduction of visceral obesity has been demonstrated to cause a drop in several pro-inflammatory chemotactic cytokines and growth factors (Bastien et al. 2015) and insulin resistance (Lottati et al. 2009) in dogs. Nonetheless, the lack of a causal link between visceral obesity and insulin resistance has also been shown in dogs (Castro et al. 2015). Further, the clinical parameters that define insulin resistance in mice and humans are not optimal measures in dogs (Ader et al. 2014). In our study, inflammatory ATM activation is associated with a moderate increase in fasting blood glucose levels, without an effect on fasting plasma insulin levels.

Despite obesity being a condition rarely occurring in the majority of mammalian species, adipose tissue is nevertheless of major importance in metabolism and the endocrine system (Szebeni et al. 2007). Our comparative study shows that adipose tissue is rich in resident immune cells in mammals and that the interplay between immune cells and adipose cells might be an evolutionary conserved trait. The results should help us to improve our understanding of the relationship between immune cells and adipose cells in mammals and are relevant for further elucidating the metabolic impact of ATMs.

Acknowledgments The authors thank Prof. Hartmut Geiger (Ulm, Germany) and his laboratory staff for providing access to flow cytometry instruments. The technical help of Renate Kunz and the editorial assistance of Livia I. Lelkes are appreciated.

References

Ader M, Stefanovski D, Richey JM, Kim SP, Kolka CM, Ionut V, Kabir M, Bergman RN (2014) Failure of homeostatic model assessment of insulin resistance to detect marked diet-induced insulin resistance in dogs. Diabetes 63:1914–1919

Ahn M, Yang W, Kim H, Jin JK, Moon C, Shin T (2012) Immunohistochemical study of arginase-1 in the spinal cords of Lewis rats with experimental autoimmune encephalomyelitis. Brain Res 1453:77–86

Amano SU, Cohen JL, Vangala P, Tencerova M, Nicoloro SM, Yawe JC, Shen Y, Czech MP, Aouadi M (2014) Local proliferation of macrophages contributes to obesity-associated adipose tissue inflammation. Cell Metab 19:162–171

Aron-Wisnewsky J, Tordjman J, Poitou C, Darakhshan F, Hugol D, Basdevant A, Aissat A, Guerre-Millo M, Clement K (2009) Human adipose tissue macrophages: m1 and m2 cell surface markers in subcutaneous and omental depots and after weight loss. J Clin Endocrinol Metab 94:4619–4623

Baldwin F, Becker AB (1993) Bronchoalveolar eosinophilic cells in a canine model of asthma: two distinctive populations. Vet Pathol 30:97–103

Basinska K, Marycz K, Śmieszek A, Nicpoń J (2015) The production and distribution of IL-6 and TNF-α in subcutaneous adipose tissue and their correlation with serum concentrations in Welsh ponies with equine metabolic syndrome. J Vet Sci 16:113–120

Bastien BC, Patil A, Satyaraj E (2015) The impact of weight loss on circulating cytokines in Beagle dogs. Vet Immunol Immunopathol 163:174–182

Bellon T, Martinez V, Lucendo B, del Peso G, Castro MJ, Aroeira LS, Rodriguez-Sanz A, Ossorio M, Sanchez-Villanueva R, Selgas R, Bajo MA (2011) Alternative activation of macrophages in human peritoneum: implications for peritoneal fibrosis. Nephrol Dial Transplant 26:2995–3005

Berg AL, Ekman K, Belak S, Berg M (2005) Cellular composition and interferon-gamma expression of the local inflammatory response in feline infectious peritonitis (FIP). Vet Microbiol 111:15–23

Bjornvad CR, Nielsen DH, Armstrong PJ, McEvoy F, Hoelmkjaer KM, Jensen KS, Pedersen GF, Kristensen AT (2011) Evaluation of a nine-point body condition scoring system in physically inactive pet cats. Am J Vet Res 72:433–437

Castro AV, Woolcott OO, Iyer MS, Kabir M, Ionut V, Stefanovski D, Kolka CM, Szczepaniak LS, Szczepaniak EW, Asare-Bediako I, Paszkiewicz RL, Broussard JL, Kim SP, Kirkman EL, Rios HC, Mkrtchyan H, Wu Q, Ader M, Bergman RN (2015) Increase in visceral fat per se does not induce insulin resistance in the canine model. Obesity (Silver Spring) 23:105–111

Cinti S (2012) The adipose organ at a glance. Dis Models Mech 5: 588–594

Chhabra P, Brayman KL (2013) Stem cell therapy to cure type 1 diabetes: from hype to hope. Stem Cells Transl Med 2:328–336

Chung S, Cuffe H, Marshall SM, McDaniel AL, Ha JH, Kavanagh K, Hong C, Tontonoz P, Temel RE, Parks JS (2014) Dietary cholesterol promotes adipocyte hypertrophy and adipose tissue inflammation in visceral, but not in subcutaneous, fat in monkeys. Arterioscler Thromb Vasc Biol 34:1880–1887

de Almeida Leal GG, Roatt BM, de Oliveira Aguiar-Soares RD, Carneiro CM, Giunchetti RC, Teixeira-Carvalho A, Martins-Filho OA, Francisco AF, Cardoso JM, Mathias FA, Correa-Oliveira R, Carneiro M, Coura-Vital W, Reis AB (2014) Immunological profile of resistance and susceptibility in naturally infected dogs by *Leishmania infantum*. Vet Parasitol 205:472–482

de Godoy MR, Swanson KS (2013) Companion animal's symposium: nutrigenomics: using gene expression and molecular biology data to understand pet obesity. J Anim Sci 91:2949–2964

Dewald O, Ren G, Duerr GD, Zoerlein M, Klemm C, Gersch C, Tincey S, Michael LH, Entman ML, Frangogiannis NG (2004) Of mice and dogs: species-specific differences in the inflammatory response following myocardial infarction. Am J Pathol 164:665–677

Dillon AR, Warner AE, Brawner W, Hudson J, Tillson M (2008) Activity of pulmonary intravascular macrophages in cats and dogs with and without adult *Dirofilaria immitis*. Vet Parasitol 158:171–176

Dupasquier M, Stoitzner P, Wan H, Cerqueira D, van Oudenaren A, Voerman JS, Denda-Nagai K, Irimura T, Raes G, Romani N, Leenen PJ (2006) The dermal microenvironment induces the expression of the alternative activation marker CD301/mMGL in mononuclear phagocytes, independent of IL-4/IL-13 signaling. J Leukoc Biol 80:838–849

Dzik JM (2014) Evolutionary roots of arginase expression and regulation. Front Immunol 5:544

Epelman S, Lavine KJ, Randolph GJ (2014) Origin and functions of tissue macrophages. Immunity 41:21–35

Ferrante AW Jr (2013) The immune cells in adipose tissue. Diabetes Obes Metab 15 (Suppl 3):34–38

Flotte TJ, Springer TA, Thorbecke GJ (1983) Dendritic cell and macrophage staining by monoclonal antibodies in tissue sections and epidermal sheets. Am J Pathol 111:112–124

Fuentes L, Röszer T, Ricote M (2010) Inflammatory mediators and insulin resistance in obesity: role of nuclear receptor signaling in macrophages. Mediators Inflamm 2010:219583

Fujimoto Y, Nakatani N, Kubo T, Semi Y, Yoshida N, Nakajima H, Iseri T, Azuma YT, Takeuchi T (2012) Adenosine and ATP affect LPS-induced cytokine production in canine macrophage cell line DH82 cells. J Vet Med Sci 74:27–34

Fujiwara S, Yasunaga S, Iwabuchi S, Masuda K, Ohno K, Tsujimoto H (2003) Cytokine profiles of peripheral blood mononuclear cells from dogs experimentally sensitized to Japanese cedar pollen. Vet Immunol Immunopathol 93:9–20

Galic S, Oakhill JS, Steinberg GR (2010) Adipose tissue as an endocrine organ. Mol Cell Endocrinol 316:129–139

Ghernati I, Corbin A, Chabanne L, Auger C, Magnol JP, Fournel C, Monier JC, Darlix JL, Rigal D (2000) Canine large granular lymphocyte leukemia and its derived cell line produce infectious retroviral particles. Vet Pathol 37:310–317

Glass CK, Olefsky JM (2012) Inflammation and lipid signaling in the etiology of insulin resistance. Cell Metab 15:635–645

Gordon S, Hamann J, Lin HH, Stacey M (2011) F4/80 and the related adhesion-GPCRs. Eur J Immunol 41:2472–2476

Gough NR, Hatem CL, Fambrough DM (1995) The family of LAMP-2 proteins arises by alternative splicing from a single gene: characterization of the avian LAMP-2 gene and identification of mammalian homologs of LAMP-2b and LAMP-2c. DNA Cell Biol 14:863–867

Grant RW, Dixit VD (2015) Adipose tissue as an immunological organ. Obesity (Silver Spring) 23:512–518

Greenberg AS, Obin MS (2006) Obesity and the role of adipose tissue in inflammation and metabolism. Am J Clin Nutr 83:461S–465S

Haase J, Weyer U, Immig K, Kloting N, Bluher M, Eilers J, Bechmann I, Gericke M (2014) Local proliferation of macrophages in adipose tissue during obesity-induced inflammation. Diabetologia 57:562–571

Hamano T, Tong V, Mutai M, Hayashi M, Tanaka E (2002) Kupffer cell-mediated cytotoxicity induced by lipopolysaccharide0111:B4 is greater in dogs than in rats and monkeys. J Toxicol Sci 27:1–9

Huynh KK, Eskelinen EL, Scott CC, Malevanets A, Saftig P, Grinstein S (2007) LAMP proteins are required for fusion of lysosomes with phagosomes. EMBO J 26:313–324

Ibisch C, Pradal G, Bach JM, Lieubeau B (2005) Functional canine dendritic cells can be generated in vitro from peripheral blood mononuclear cells and contain a cytoplasmic ultrastructural marker. J Immunol Methods 298:175–182

Ionut V, Liu H, Mooradian V, Castro AV, Kabir M, Stefanovski D, Zheng D, Kirkman EL, Bergman RN (2010) Novel canine models of obese prediabetes and mild type 2 diabetes. Am J Physiol Endocrinol Metab 298:E38–E48

Janckila AJ, Slone SP, Lear SC, Martin A, Yam LT (2007) Tartrate-resistant acid phosphatase as an immunohistochemical marker for inflammatory macrophages. Am J Clin Pathol 127:556–566

Kaku Y, Imaoka H, Morimatsu Y, Komohara Y, Ohnishi K, Oda H, Takenaka S, Matsuoka M, Kawayama T, Takeya M, Hoshino T (2014) Overexpression of CD163, CD204 and CD206 on alveolar macrophages in the lungs of patients with severe chronic obstructive pulmonary disease. PLoS One 9:e87400

Kambara K, Ohashi W, Tomita K, Takashina M, Fujisaka S, Hayashi R, Mori H, Tobe K, Hattori Y (2015) In vivo depletion of CD206(+) M2 macrophages exaggerates lung injury in endotoxemic mice. Am J Pathol 185:162–171

Kass M, Witkin A, Terzopoulos D (1988) Snakes: active contour models. Int J Comput Vis 1:321–331

Kearns RJ, Hayek MG, Turek JJ, Meydani M, Burr JR, Greene RJ, Marshall CA, Adams SM, Borgert RC, Reinhart GA (1999) Effect of age, breed and dietary omega-6 (n-6): omega-3 (n-3) fatty acid ratio on immune function, eicosanoid production, and lipid peroxidation in young and aged dogs. Vet Immunol Immunopathol 69:165–183

Kim AY, Kim HS, Kang JH, Yang MP (2015) Serum adipokine concentrations in dogs with diabetes mellitus: a pilot study. J Vet Sci (in press)

Kim SK, Shin MS, Jung BK, Shim JY, Won HS, Lee PR, Kim A (2006) Effect of dehydroepiandrosterone on lipopolysaccharide-induced interleukin-6 production in DH82 cultured canine macrophage cells. J Reprod Immunol 70:71–81

Kipar A, Baptiste K, Meli ML, Barth A, Knietsch M, Reinacher M, Lutz H (2005) Age-related dynamics of constitutive cytokine transcription levels of feline monocytes. Exp Gerontol 40:243–248

Klocke NW, Snyder PW, Widmer WR, Zhong W, McCabe GP, Breur GJ (2005) Detection of synovial macrophages in the joint capsule of dogs with naturally occurring rupture of the cranial cruciate ligament. Am J Vet Res 66:493–499

Kurzman ID, Shi F, Vail DM, MacEwen EG (1999) In vitro and in vivo enhancement of canine pulmonary alveolar macrophage cytotoxic activity against canine osteosarcoma cells. Cancer Biother Radiopharm 14:121–128

Lee BC, Lee J (2014) Cellular and molecular players in adipose tissue inflammation in the development of obesity-induced insulin resistance. Biochim Biophys Acta 1842:446–462

Lee SJ, Evers S, Roeder D, Parlow AF, Risteli J, Risteli L, Lee YC, Feizi T, Langen H, Nussenzweig MC (2002) Mannose receptor-mediated regulation of serum glycoprotein homeostasis. Science 295:1898–1901

Li P, Spann NJ, Kaikkonen MU, Lu M, da Oh Y, Fox JN, Bandyopadhyay G, Talukdar S, Xu J, Lagakos WS, Patsouris D, Armando A, Quehenberger O, Dennis EA, Watkins SM, Auwerx J, Glass CK, Olefsky JM (2013) NCoR repression of LXRs restricts macrophage biosynthesis of insulin-sensitizing omega 3 fatty acids. Cell 155:200–214

Lottati M, Kolka CM, Stefanovski D, Kirkman EL, Bergman RN (2009) Greater omentectomy improves insulin sensitivity in nonobese dogs. Obesity (Silver Spring) 17:674–680

Loukas A, Doedens A, Hintz M, Maizels RM (2000) Identification of a new C-type lectin, TES-70, secreted by infective larvae of *Toxocara canis*, which binds to host ligands. Parasitology 121:545–554

Lumeng CN, Bodzin JL, Saltiel AR (2007) Obesity induces a phenotypic switch in adipose tissue macrophage polarization. J Clin Invest 117:175–184

Marx C, Silveira MD, Beyer Nardi N (2015) Adipose-derived stem cells in veterinary medicine: characterization and therapeutic applications. Stem Cells Dev 24:803–813

Medbury HJ, James V, Ngo J, Hitos K, Wang Y, Harris DC, Fletcher JP (2013) Differing association of macrophage subsets with atherosclerotic plaque stability. Int Angiol 32:74–84

Menendez-Gutierrez MP, Röszer T, Fuentes L, Nunez V, Escolano A, Redondo JM, De Clerck N, Metzger D, Valledor AF, Ricote M (2015) Retinoid X receptors orchestrate osteoclast differentiation and postnatal bone remodeling. J Clin Invest 125:809–23

Mielcarek M, Kucera KA, Nash R, Torok-Storb B, McKenna HJ (2007) Identification and characterization of canine dendritic cells generated in vivo. Biol Blood Marrow Transplant 13:1286–1293

Módis L (1974) Topo-optical investigations of mucopolysaccharides (acid glycosaminoglycans). In: Graumann W, Neumann K (eds) Handbuch der Histochemie: Polysaccharides, vol 11/4. Fischer, Stuttgart, pp S11–S15

Mori S, Kiuchi S, Ouchi A, Hase T, Murase T (2014) Characteristic expression of extracellular matrix in subcutaneous adipose tissue development and adipogenesis; comparison with visceral adipose tissue. Int J Biol Sci 10:825–833

Morris DL, Oatmen KE, Wang T, DelProposto JL, Lumeng CN (2012) CX3CR1 deficiency does not influence trafficking of adipose tissue macrophages in mice with diet-induced obesity. Obesity (Silver Spring) 20:1189–1199

Müller L, Kollar E, Balogh L, Postenyi Z, Marian T, Garai I, Balkay L, Trencsenyi G, Thuroczy J (2014) Body fat distribution and metabolic consequences—examination opportunities in dogs. Acta Vet Hung 62:169–179

Munder M (2009) Arginase: an emerging key player in the mammalian immune system. Br J Pharmacol 158:638–651

Munder M, Eichmann K, Moran JM, Centeno F, Soler G, Modolell M (1999) Th1/Th2-regulated expression of arginase isoforms in murine macrophages and dendritic cells. J Immunol 163:3771–3777

Munder M, Schneider H, Luckner C, Giese T, Langhans CD, Fuentes JM, Kropf P, Mueller I, Kolb A, Modolell M, Ho AD (2006) Suppression of T-cell functions by human granulocyte arginase. Blood 108:1627–1634

Murray PJ, Allen JE, Biswas SK, Fisher EA, Gilroy DW, Goerdt S, Gordon S, Hamilton JA, Ivashkiv LB, Lawrence T, Locati M, Mantovani A, Martinez FO, Mege JL, Mosser DM, Natoli G, Saeij JP, Schultze JL, Shirey KA, Sica A, Suttles J, Udalova I, van Ginderachter JA, Vogel SN, Wynn TA (2014) Macrophage activation and polarization: nomenclature and experimental guidelines. Immunity 41:14–20

Osborn O, Olefsky JM (2012) The cellular and signaling networks linking the immune system and metabolism in disease. Nat Med 18:363–374

Paek HJ, Kim C, Williams SK (2014) Adipose stem cell-based regenerative medicine for reversal of diabetic hyperglycemia. World J Diabetes 5:235–243

Panaro MA, Acquafredda A, Lisi S, Lofrumento DD, Mitolo V, Sisto M, Fasanella A, Trotta T, Bertani F, Consenti B, Brandonisio O (2001) Nitric oxide production by macrophages of dogs vaccinated with killed *Leishmania infantum promastigotes*. Comp Immunol Microbiol Infect Dis 24:187–195

Pavelka M, Roth J (2010) Lysosomes: localisation of acid phosphatase, lamp and polylactosamine. Functional ultrastructure. Springer, Vienna

Ponti W, Rubino T, Bardotti M, Poli G, Parolaro D (2001) Cannabinoids inhibit nitric oxide production in bone marrow derived feline macrophages. Vet Immunol Immunopathol 82:203–214

Porcheray F, Viaud S, Rimaniol AC, Leone C, Samah B, Dereuddre-Bosquet N, Dormont D, Gras G (2005) Macrophage activation switching: an asset for the resolution of inflammation. Clin Exp Immunol 142:481–489

Pucheu-Haston CM, Santoro D, Bizikova P, Eisenschenk MN, Marsella R, Nuttall T (2015) Review: Innate immunity, lipid metabolism and nutrition in canine atopic dermatitis. Vet Dermatol 26:104–e28

Qiu Y, Nguyen KD, Odegaard JI, Cui X, Tian X, Locksley RM, Palmiter RD, Chawla A (2014) Eosinophils and type 2 cytokine signaling in macrophages orchestrate development of functional beige fat. Cell 157:1292–1308

Ricklin Gutzwiller ME, Moulin HR, Zurbriggen A, Roosje P, Summerfield A (2010) Comparative analysis of canine monocyte- and bone-marrow-derived dendritic cells. Vet Res 41:40

Rodrigues GC, Oliveira LJ, Monteiro JM, Lima AR, Gonçalez PO, Hernandez-Blazquez FJ, Leiser R, Kfoury JR Jr (2010) Ultrastructural characterization of bovine umbilical cord blood cells. Pesqui Vet Bras 30:897–902

Rosen ED, Spiegelman BM (2014) What we talk about when we talk about fat. Cell 156:20–44

Röszer T (2012) Phagosomal and lysosomal NO synthesis. In: Röszer T (ed) The biology of subcellular nitric oxide. Springer, Heidelberg, pp 145–155

Röszer T (2014) The invertebrate midintestinal gland ("hepatopancreas") is an evolutionary forerunner in the integration of immunity and metabolism. Cell Tissue Res 358:685–695

Röszer T (2015) Understanding the mysterious M2 macrophage through activation markers and effector mechanisms. Mediat Inflamm 2015:16

Röszer T, Menendez-Gutierrez MP, Lefterova MI, Alameda D, Nunez V, Lazar MA, Fischer T, Ricote M (2011) Autoimmune kidney disease and impaired engulfment of apoptotic cells in mice with macrophage peroxisome proliferator-activated receptor gamma or retinoid X receptor alpha deficiency. J Immunol 186:621–631

Röszer T, Menendez-Gutierrez MP, Cedenilla M, Ricote M (2013) Retinoid X receptors in macrophage biology. Trends Endocrinol Metab 24:460–468

Sanches FP, Tomokane TY, Da Matta VL, Marcondes M, Corbett CE, Laurenti MD (2014) Expression of inducible nitric oxide synthase in macrophages inversely correlates with parasitism of lymphoid tissues in dogs with visceral leishmaniasis. Acta Vet Scand 56:57

Shaul ME, Bennett G, Strissel KJ, Greenberg AS, Obin MS (2010) Dynamic, M2-like remodeling phenotypes of CD11c+ adipose tissue macrophages during high-fat diet-induced obesity in mice. Diabetes 59:1171–1181

Shi F, Kurzman ID, MacEwen EG (1995) In vitro and in vivo production of interleukin-6 induced by muramyl peptides and lipopolysaccharide in normal dogs. Cancer Biother 10:317–325

Spitzbarth I, Bock P, Haist V, Stein VM, Tipold A, Wewetzer K, Baumgartner W, Beineke A (2011) Prominent microglial activation in the early proinflammatory immune response in naturally occurring canine spinal cord injury. J Neuropathol Exp Neurol 70: 703–714

Staines K, Hunt LG, Young JR, Butter C (2014) Evolution of an expanded mannose receptor gene family. PLoS One 9:e110330

Steinbach F, Stark R, Ibrahim S, Gawad EA, Ludwig H, Walter J, Commandeur U, Mauel S (2005) Molecular cloning and characterization of markers and cytokines for equid myeloid cells. Vet Immunol Immunopathol 108:227–236

Svensson-Arvelund J, Mehta RB, Lindau R, Mirrasekhian E, Rodriguez-Martinez H, Berg G, Lash GE, Jenmalm MC, Ernerudh J (2015) The human fetal placenta promotes tolerance against the semiallogeneic fetus by inducing regulatory T cells and homeostatic M2 macrophages. J Immunol 194:1534–1544

Szebeni J, Alving CR, Rosivall L, Bunger R, Baranyi L, Bedocs P, Toth M, Barenholz Y (2007) Animal models of complement-mediated hypersensitivity reactions to liposomes and other lipid-based nanoparticles. J Liposome Res 17:107–117

Taglinger K, Day MJ, Foster AP (2007) Characterization of inflammatory cell infiltration in feline allergic skin disease. J Comp Pathol 137: 211–223

Taglinger K, Van Nguyen N, Helps CR, Day MJ, Foster AP (2008) Quantitative real-time RT-PCR measurement of cytokine mRNA expression in the skin of normal cats and cats with allergic skin disease. Vet Immunol Immunopathol 122:216–230

Titos E, Rius B, Gonzalez-Periz A, Lopez-Vicario C, Moran-Salvador E, Martinez-Clemente M, Arroyo V, Claria J (2011) Resolvin D1 and its precursor docosahexaenoic acid promote resolution of adipose tissue inflammation by eliciting macrophage polarization toward an M2-like phenotype. J Immunol 187:5408–5418

Tsuji W, Rubin JP, Marra KG (2014) Adipose-derived stem cells: implications in tissue regeneration. World J Stem Cells 6:312–321

Turchetti AP, da Costa LF, Romao Ede L, Fujiwara RT, da Paixao TA, Santos RL (2015) Transcription of innate immunity genes and cytokine secretion by canine macrophages resistant or susceptible to intracellular survival of *Leishmania infantum*. Vet Immunol Immunopathol 163:67–76

Van de Velde H, Janssens GP, de Rooster H, Polis I, Peters I, Ducatelle R, Nguyen P, Buyse J, Rochus K, Xu J, Verbrugghe A, Hesta M (2013) The cat as a model for human obesity: insights into depot-specific inflammation associated with feline obesity. Br J Nutr 110: 1326–1335

Verbrugghe A, Janssens GP, Van de Velde H, Cox E, De Smet S, Vlaeminck B, Hesta M (2014) Failure of a dietary model to affect markers of inflammation in domestic cats. BMC Vet Res 10:104

Weisberg SP, McCann D, Desai M, Rosenbaum M, Leibel RL, Ferrante AW (2003) Obesity is associated with macrophage accumulation in adipose tissue. J Clin Invest 112:1796–1808

West M (2009) Dead adipocytes and metabolic dysfunction: recent progress. Curr Opin Endocrinol Diabetes Obes 16:178–182

Williamson JR, Grisham JW (1961) Electron microscopy of leukocytic margination and emigration in acute inflammation in dog pancreas. Am J Pathol 39:239–256

Yamate J, Yoshida H, Tsukamoto Y, Ide M, Kuwamura M, Ohashi F, Miyamoto T, Kotani T, Sakuma S, Takeya M (2000) Distribution of cells immunopositive for AM-3K, a novel monoclonal antibody recognizing human macrophages, in normal and diseased tissues of dogs, cats, horses, cattle, pigs, and rabbits. Vet Pathol 37:168–176

Zeyda M, Farmer D, Todoric J, Aszmann O, Speiser M, Gyori G, Zlabinger GJ, Stulnig TM (2007) Human adipose tissue macrophages are of an anti-inflammatory phenotype but capable of excessive pro-inflammatory mediator production. Int J Obes (Lond) 31:1420–1428

Zhang LJ, Guerrero-Juarez CF, Hata T, Bapat SP, Ramos R, Plikus MV, Gallo RL (2015) Innate immunity. Dermal adipocytes protect against invasive *Staphylococcus aureus* skin infection. Science 347:67–71